

Loss of wind power for wind turbines due to an upstream hill

B. Ruck, R. Boes, M. Gruber

Abstract—In advance of the implementation of wind turbines, a profitability forecast must be performed allowing an economical assessment of the project. For a detailed analysis of the wind potential, wind climate data of the site are required. In most cases, however, these data do not exist and it is necessary to rely on data from remote stations, which are 'extrapolated' numerically to the site. This numerical extrapolation is critical and in debate, especially, when orographically structured terrain is present. In order to complement and to validate existing numerical programs, an experimental investigation in an atmospheric boundary layer tunnel has been carried out, delivering detailed information on the influence of upstream hills on the wind power potential for wind turbines. Special emphasis was laid on the case where wind turbine height and hill height are in the same order of magnitude. Depending on factors of influence, exposure coefficients could be determined, which account for the loss of wind power due to the upstream hill.

Keywords—Wind turbine, upstream hill, wind power loss, orographically structured terrain

I. INTRODUCTION

INCREASINGLY, wind turbines are installed in orographically structured terrain. To assess the efficiency of a wind turbine and to estimate the annual energy production, the wind climatology at the turbine location must be known. Unfortunately, the site-specific wind data are not known in most cases, so that wind data from remote weather stations are taken and 'extrapolated' by flow models to the wind turbine site ('micro-siting'). For this purpose, flow models of different type are used. Linear flow models [1,2] compute the wind climatology by parameterizing relevant factors of influence (surface roughness, site-near obstacle dimensions, height contour lines of terrain). However, the incorporated orographic flow model [3] can be applied only to neutrally stable wind flows over gently sloping terrain and low hills. In rugged or complex terrain, linear flow models show well-known limitations e.g. overestimating wind speed-up [4,5,6]. In contrast to linear models, 3-D nonlinear flow models [7] compute the 3-D wind field

with input data from a digital terrain model, a roughness map and from wind climatology data derived from at least one met station within the modeled area. The wind field computation is based on the solution of the time-averaged Navier-Stokes equations (RANS = Reynolds-averaged Navier-Stokes equations). To close the system of equations, the k- ϵ turbulence model is used in most of these non-linear flow models. However, it is known from various fields of fluid research that RANS models tend to overestimate turbulent kinetic energy and to underestimate mean flow recirculation zones and often lead to uncertainties when large-scale turbulent transport phenomena or sharp bends in the flow field are present [8,9]. More sophisticated or even time-resolved flow computations with Large Eddy Simulation (LES) or Direct Numerical Simulation (DNS) are either not practical for industrial use because of their costs or not feasible because of their physical limitation (transition not predictable, Reynolds numbers too high).

As reported in literature, 3-D nonlinear flow models show better agreement with mast measurements than results obtained with linear models. However, independent studies on this subject [10] are rare and indicate that terrain complexity can generate substantial modeling uncertainties obviously with both model types. Thus, the question how accurate the wind energy resources can be estimated for a specific location in orographically structured terrain cannot easily be answered by existing commercial wind resource assessment programs

As a consequence of the shortcomings of software-based models, it seems that physical modeling in an atmospheric boundary layer wind tunnel can deliver more detailed and realistic data on wind power density loss in hilly terrain, where wind field conditions are characterized by specific orographically generated turbulence and wind profile properties.

II. THE FLOW ACROSS HILLS

The importance of mountain flows increased in the 1950s and 1960s with the growing interest in wind engineering, see e.g. [11]. In the following decades, different numerical models have been developed in order to predict the turbulent flow over hills [3,12,13]. Quite a number of field measuring campaigns followed delivering data that could be compared with these models, see e.g. [14-16].

Wind tunnel studies revealed and specified mean flow and turbulent properties of the flow delivering more detailed data on flow separation in the lee of the hill or on the influence of canopy roughness [17-20]. Boundary layer wind tunnel studies

B. Ruck, R. Boes and M. Gruber are with the Laboratory of Building- and Environmental Aerodynamics (IfH) at the Karlsruhe Institute of Technology (KIT), 76131 Karlsruhe, Germany (corresponding author phone: +49 721 608 43897, e-mail: ruck@kit.edu).

on the flow across forested hills, see [21,22], showed that a vegetation cover triggers flow separation even in the case of low hills. It could also be shown that the onset of the separation zone in the lee of a hill depends on the ratio of boundary layer thickness to the hill height δ/H , the shape of the hill (slope) and the surface roughness [23]. There is no doubt that orography exerts a great influence on instant, time-averaged or climatologic wind speed at a given site. Thus, in mountainous regions, the wind energy production of wind turbines is in most cases smaller than in the plane countryside.

Summarizing the existing knowledge of wind flow over (smooth) hills shows that the great number of theoretical, numerical and experimental studies in the last decades have provided the fluid mechanical fundamentals, which are so far well known. Concerning wind energy applications, however, the interaction of orographically structured terrain, forested surfaces and wind turbines is not fully understood. This is partially due to the fact that most models treat vegetation as a pure roughness problem, however, it must be realized that 'permeability' of the forest canopy should not be mistaken as pure 'roughness'. Permeability enables mean and turbulent fluxes not only in one but in all directions. Additionally, atmospheric stability [24] plays an important role.

Another today's problem associated with wind energy application in hilly terrain is that due to political directives and supports schemes [25] wind turbines shall be erected also in low wind areas of hilly terrain. However, in many cases, the annual-averaged wind velocities in those areas are so low that profitability of the project can hardly be achieved (annual-averaged wind velocity is almost equal to the profitability onset velocity). Profitability forecasts for those areas based on numerical assessments deliver often only a very slight profitability of the project, which decides on its implementation. However, to decide upon the erection of wind turbines on the basis of such numerical assessment is in many cases negligent, since meteorologists/engineers involved in numerical determination of on-site velocity data admit frankly that the accuracy of their wind velocity calculation in orographically structured terrain is plus/minus 1 m/sec. Compared to an annual-averaged wind velocity in low wind areas of about 5 m/sec, this yields an uncertainty of plus/minus 20 %. However, a fluctuation of 20 % in wind velocity results in a fluctuation of wind power of about plus/minus 50 % ! In other words, if a numerical assessment of a project in hilly terrain delivers the conclusion that the point of beginning profitability is just reached or exceeded only by a small amount, this means that the project fails economically with a probability of about 50% (equal probability of exceedance and fall below of the profitability onset velocity provided) - who would like to invest in such a project? In this context, it is most interesting to have other and possibly safer sources of assessment like the physical modeling in atmospheric boundary layer wind tunnels.

In the following, a base configuration of wind energy application in hilly terrain - the interaction of a wind turbine and an

upstream hill - is investigated in an atmospheric boundary layer wind tunnel study, see Fig. 1.

III. EXPERIMENTAL DETAILS

A. Boundary layer Simulation

The use of atmospheric boundary layer wind tunnels to investigate wind flows over complex and forested terrain is well established in building- and environmental aerodynamics [26-30]. For the investigations presented here, the simulation of an atmospheric boundary layer in the wind tunnel was realized according to the criteria given in Table 1. Simulation and measurements of the flow field were carried out in the atmospheric boundary layer wind tunnel (length 29 m) of the Laboratory of Building- and Environmental Aerodynamics at KIT. This constant pressure wind tunnel has a closed recirculation and an octagonal cross-section with a width of 1.5 m. The test section is divided into a 4 m long fetch needed for the formation of the boundary layer and a 4 m long measuring section in which the boundary layer with a height of about 0.55 m is almost constant.

- wind profil exponent

$$\alpha_{\text{model}} = \alpha_{\text{full scale}} \quad (1)$$

- geometry

$$\frac{Z_{0,\text{model}}}{Z_{0,\text{full scale}}} = M \quad (2)$$

- turbulence intensity

$$I_{u,\text{model}}(z) = I_{u,\text{full scale}}(z) \quad (3)$$

- turbulent spectrum

$$\left(\frac{f \cdot S_{uu}(f)}{\sigma_u^2} \right)_{\text{model}} = \left(\frac{f \cdot S_{uu}(f)}{\sigma_u^2} \right)_{\text{full scale}} \quad (4)$$

- turbulent length scale

$$\frac{L_{u,\text{model}}(z)}{L_{u,\text{full scale}}(z)} = M \quad (5)$$

- roughness Reynolds number

$$\text{Re}_{R,\text{model}} = \frac{u_* \cdot Z_{0,\text{model}}}{\nu} > 5 \quad (6)$$

Table. 1: Similarity criteria for the boundary layer simulation

B. Flow measurement technique

For the flow measurements, a two-dimensional LDA system was used, whose properties are listed in Table 2. It uses an

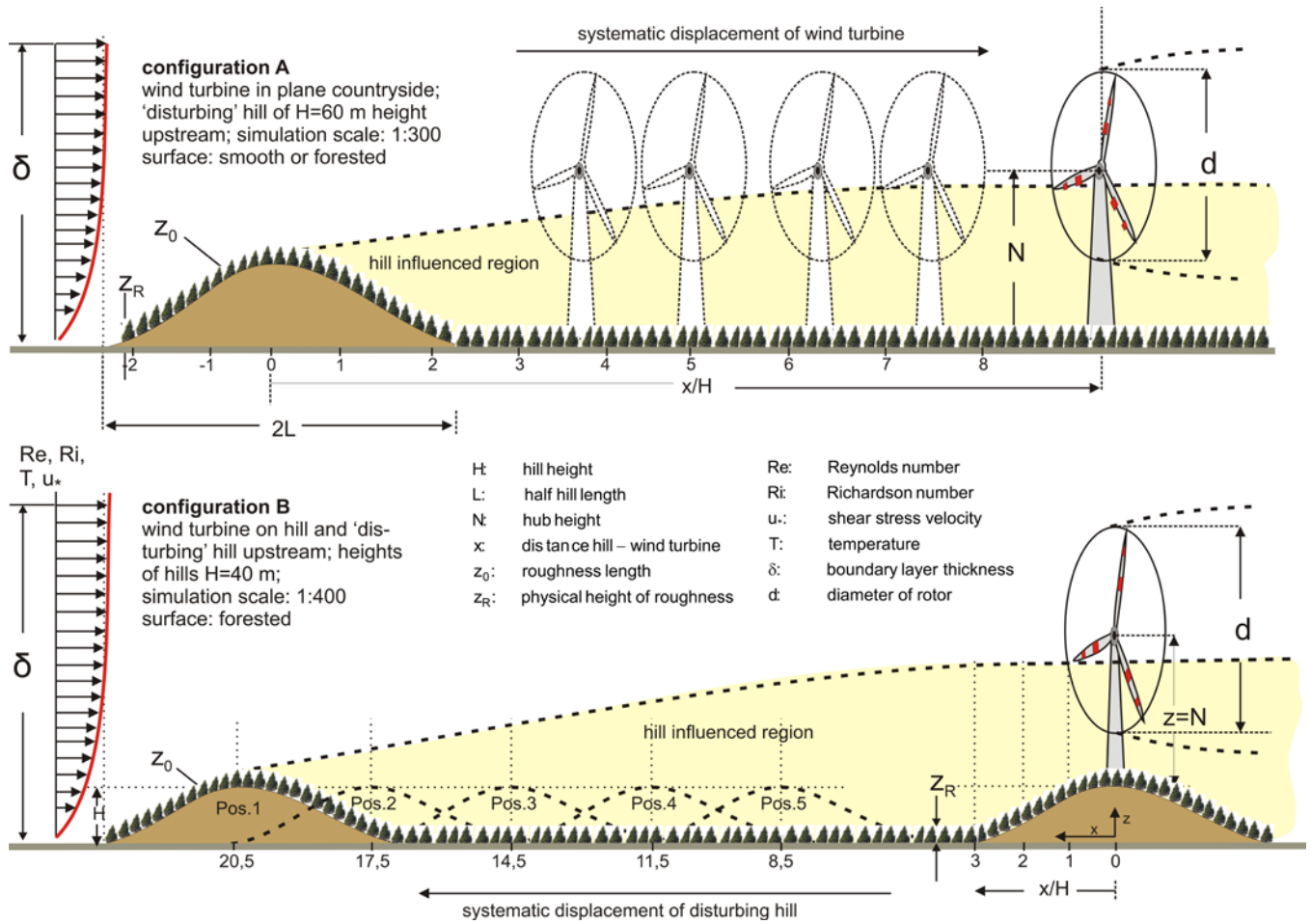


Fig. 1: Investigated configurations in the atmospheric boundary layer wind tunnel

argon-ion laser with a power of 4 watts (manufacturer: Coherent, model Innova 90) as light source. The system operates in dual-beam mode. Fig. 2 shows a photo of the 2D-LDA system used during the measurement process. Two double Bragg cells (TSI ColorBurst) were used for the frequency shift of the par-

tial beams. The scattered light was detected in forward direction by a photomultiplier unit (TSI; Color Link). The data processing was performed with two TSI signal processors (Model IFA 550).



Fig. 2: 2D-LDA system for flow measurements

LDA-system properties	u-component (green)	v- component (blue)
wave length λ	515 nm	488 nm
max. light power	3 W	3 W
frequency shift	0.60 MHz	0.75 MHz
focal length	1.5 m	1.5 m
half angle φ of crossing beams	0.955°	0.955°
fringe spacing Δx	$15.42 \mu\text{m}$	$14.64 \mu\text{m}$
number n of fringes	51	52

Table.2: Properties of LDA-system

C. Hill modeling

The two-dimensional model hills (scale 1:300 for configuration A and scale 1:400 for configuration B) were made of plywood and had a cosine shape according to:

$$z_h(x) = H \cdot \cos^2\left(\frac{\pi \cdot x}{2 \cdot L}\right) \quad -L < x < L \quad (7)$$

The length L is defined as the distance between the foot and the top of the hill. After the wooden construction was completed, the surface of the hill was covered with a layer of styrofoam.

To simulate the forest vegetation, tree models were inserted into the Styrofoam layer, which had a height of approximately 5.5 cm in height. Their shape was conical like spruce trees that do not grow under light stress condition. The simulated tree density corresponded to a very loose forest vegetation with approximately 60 trees per ha. The pressure loss of the crown material was about 200 m^{-1} , which corresponds to a pressure loss of 0.7 m^{-1} in nature. Details for the simulation of forest vegetation for wind tunnel studies can be found in [29]. It was not the aim of this investigation to reproduce a natural forest canopy in all details but to ensure the aerodynamic property of a fully rough canopy surface.

D. Wind power calculation and exposure coefficient

The wind power computed with the mean horizontal wind velocity u , which falls onto the rotor swept area is obtained via the solution of the integral (8), see Fig. 3 for notation, characterizes the wind energy content.

$$\begin{aligned} P(N,r) &= \frac{1}{2} \cdot \int_{z=(N-r)}^{z=(N+r)} \rho \cdot u^3(z) \cdot s(z) \cdot dz \\ &= \int_{z=(N-r)}^{z=(N+r)} \rho \cdot u^3(z) \cdot \sqrt{r^2 - (N-z)^2} \cdot dz \end{aligned} \quad (8)$$

The maximum energy content available for wind turbines can be computed by multiplying equation (8) with the Betz constant of 0.59. If the velocity field is disturbed by an upstream hill, the wind energy content depends on the streamwise position x behind the hill, the hill height H , the hub height N and the rotor swept area diameter r .

$$P(N,r,x,H) = \frac{1}{2} \cdot \int_{z_0=(N-r)}^{z_1=(N+r)} \rho \cdot u^3(x,z) \cdot s(z) \cdot dz \quad (9)$$

Referring the wind power for a given hub height and swept area diameter behind an upstream hill to the corresponding wind power in the undisturbed approach flow before the

disturbing hill delivers an exposure coefficient, which quantifies the decrease or increase of wind power due to the hill.

$$\varepsilon_H(N,r,x,H) = \frac{P_{\text{after}}(N,r,x,H)}{P_{\text{before}}(N,r)} \quad (10)$$

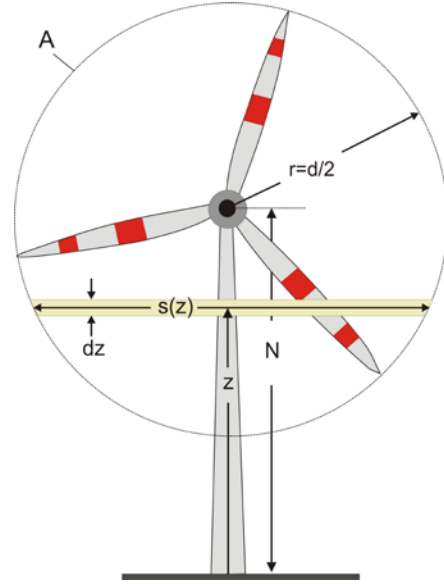


Fig. 3: Notation for wind power computation

IV. RESULTS CONFIGURATION A

Figure 4 shows the exposure coefficient for a wind turbine with rotor diameter of 90 m. As can be inferred from Fig. 4, the distance from the wind turbine to the upstream hill plays an important role for the available wind power. The interpretation of the curves in Figure 4 is easy, because each curve refers to a fixed and specified distance between wind turbine and hill. Going upwards along a curve means that at the same distance from the hill the hub height is pushed upwards, which increases the exposure coefficient in most cases.

Comparing Fig. 4 top with Fig. 4 bottom reveals that forested surfaces of hill and surrounding land induce a significant loss of wind power when compared to smooth surfaces. For a wind turbine with hub height of 120 m with rotor diameter of 90 m and at position $x/H=7.5$, the wind power loss amounts to 23% and for a wind turbine with the same rotor diameter but a hub height of 90 m the wind power loss amounts to 49%. When compared to the undisturbed approach flow without hill, the loss in wind power for the forested case is for the 120 hub height 29% and for the 90 m hub height 56%.

This clearly shows that even at a hub height of 120 m the forest canopy exerts a strong influence on the available wind power and underlines that the only chance to keep the wind power losses induced by the forested green cover on a low level is to increase the hub height significantly.

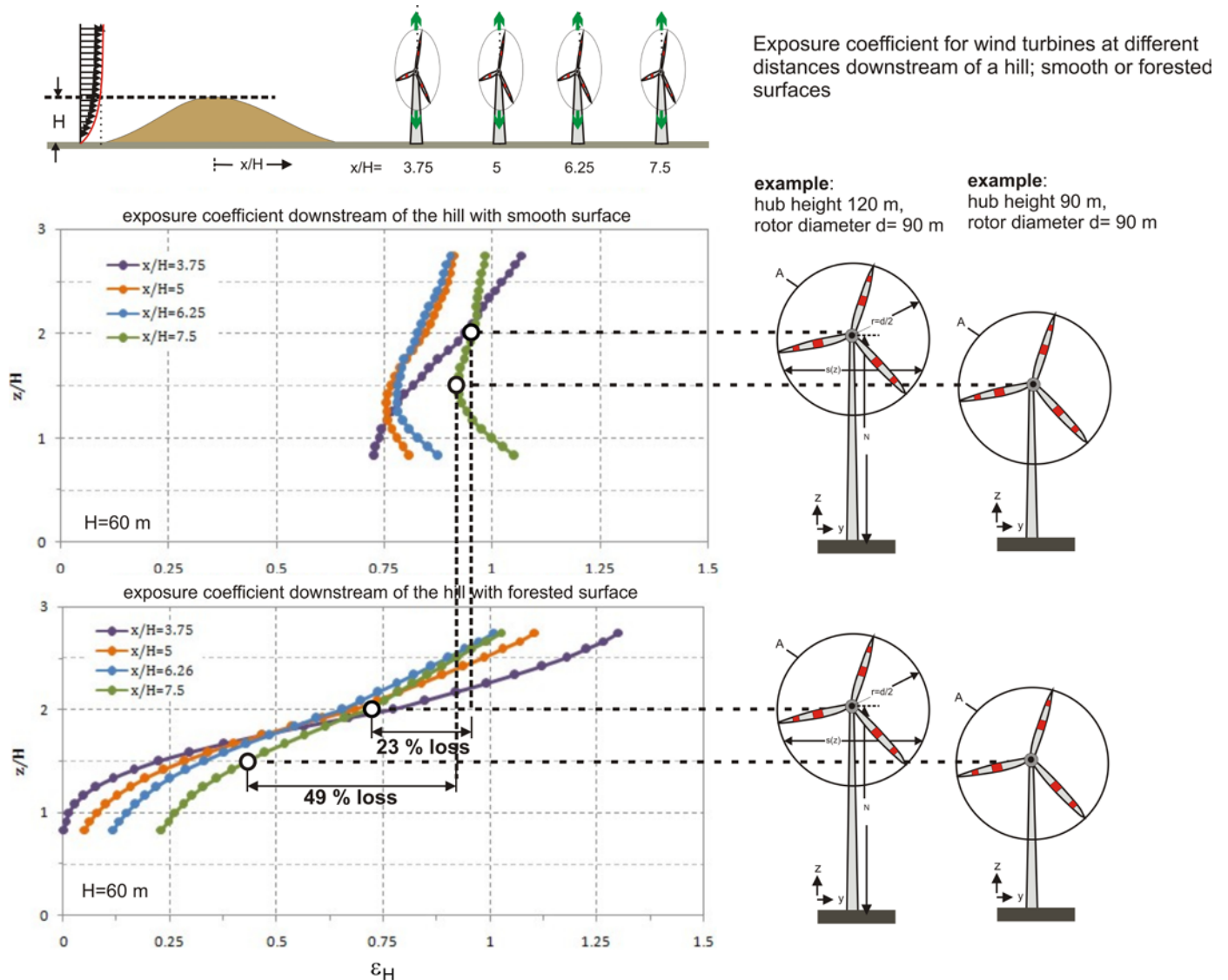


Fig. 4: Exposure coefficients ϵ_H measured at different distances from the disturbing upstream hill (height 60 m) for varying hub heights and fixed rotor diameter of 90 m; top: smooth surfaces; bottom: forested surfaces with tree density of 60 tree/ha, tree height 16.5 m; permeability of crown material 0.7 m^{-1} ; losses demonstrated (dashed lines) for distance $x/H=7.5$ and hub heights of 90 m and 120 m

As can be seen, the exposure coefficient can obtain values greater than 1 or less than 1 denoting hub positions, where an increase or decrease of wind power is induced by the hill. Exposure coefficients greater than 1 are caused by the deflection of air by the hill leading to an overspeed outside of the wake zone whereas exposure coefficients less than 1 stem from the fact that at least a part of the rotor swept area is located in the wake zone of the hill.

For the forested hill and for the investigated range of distance $3.75 \leq x/H \leq 7.5$, see Fig. 4 bottom, one can conclude that as long as the hub height is below about two times the hill height, the exposure coefficient increases with increasing distance of the wind turbine from the hill. Apparently, this zone

is dominated by the wake, whose influence fades with increasing distance. For hub heights higher than about two times the hill height, this tendency turns into the opposite and the exposure coefficients increase with decreasing distance of the wind turbine from the hill. The latter is due to the aforementioned flow displacement effect of the hill.

In Fig. 5, similar results are given for a rotor diameter of 70 m. As can be inferred, the differences when compared to the results given in Fig. 4 are rather small. Exemplarily, for a wind turbine with hub height of 120 m with rotor diameter of 70 m and at position $x/H=7.5$, the wind power loss amounts to 24% and for a wind turbine with the same rotor diameter but a hub height of 90 m the wind power loss amounts to 50%. When

compared to the undisturbed approach flow without hill, the loss in wind power for the forested case is for the 120 m hub height 29% and for the 90 m hub height 58%. Also in Fig. 5 we see that as long as the hub height is below about two times the hill height, the exposure coefficient increases with increasing distance of the wind turbine from the hill, whereas it decreases for hub height above about two hill heights.

Furthermore, the comparison of the results of Fig. 4 and 5 reveals that the exposure coefficient does not 'significantly' depend on the rotor diameter. Of course, between the exposure coefficients for rotor diameter 90 m and 70 m there are some small differences, however, significant changes are not

registered. However, one should be cautious with the interpretation of this fact, which states only that the exposure coefficients (ratio of wind power before and behind the hill) does not significantly depend on the rotor swept area. Of course, from an absolute point of view, the wind power is always proportional to the rotor swept area.

A bigger rotor diameter better integrates over the differences of the flow field, and in turn, a smaller better reproduces changes of the flow field, which can be inferred from a comparison of Fig. 4 bottom with Fig. 5 bottom, where the curves for different turbine positions from the hill do faster adopt (bend) for the smaller rotor diameter.

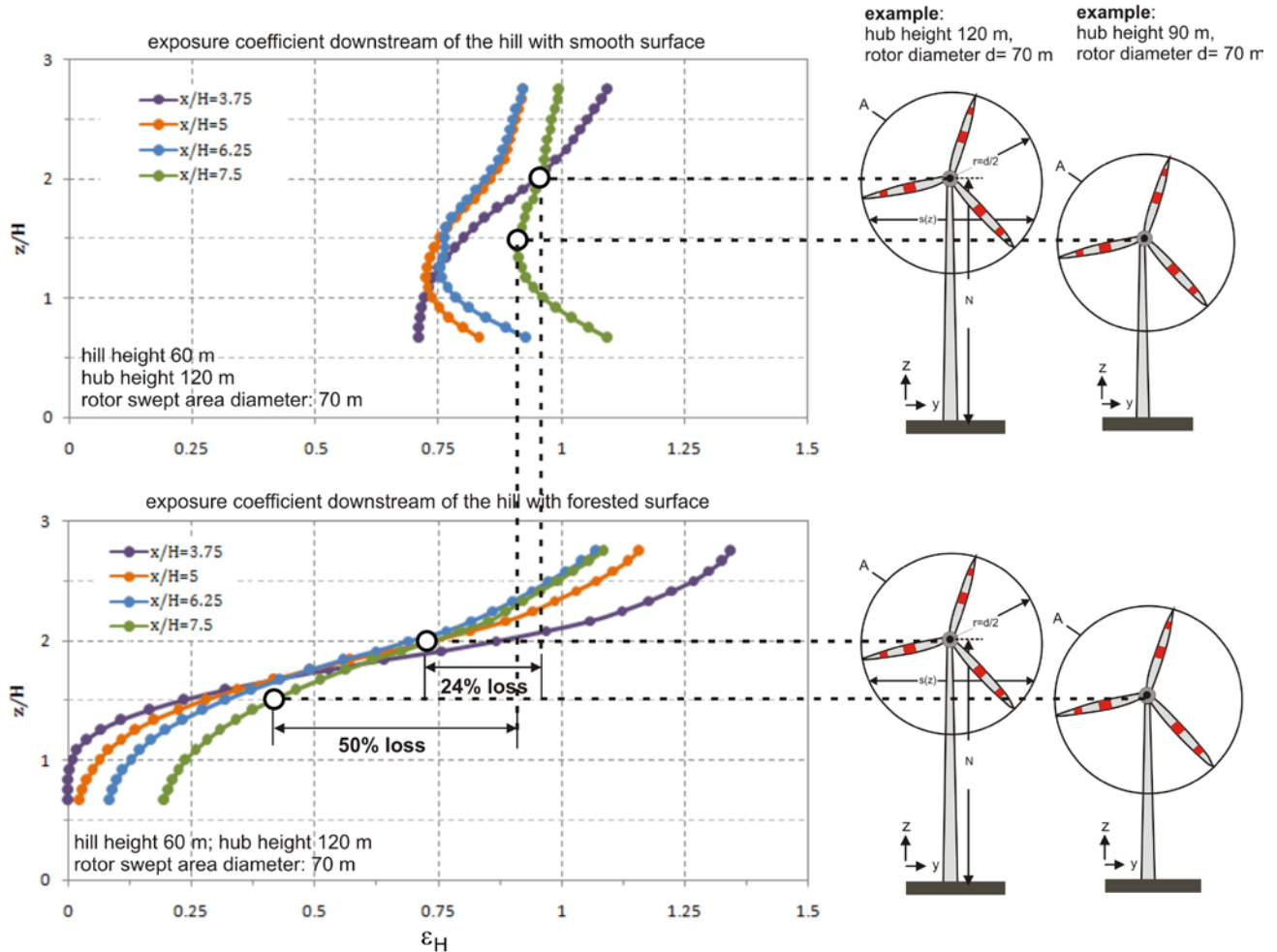


Fig. 5: Exposure coefficients ϵ_H measured at different distances from the disturbing upstream hill (height 60 m) for varying hub heights and fixed rotor diameter of 70 m; top: smooth surfaces; bottom: forested surfaces with tree density of 60 tree/ha, tree height 16.5 m; permeability of crown material 0.7 m^{-1} ; losses demonstrated (dashed lines) for distance $x/H=7.5$ and hub heights of 90 m and 120 m

Each curve in Fig. 4 and 5 represents a fixed distance of the turbine from the hill. Instead of displaying the value of the exposure coefficients on the abscissa, one can represent them by color coding. Thus, one can calculate the exposure coefficients for all possible positions and display the values in an isoplot, see Fig. 6., where the exposure coefficients for

smooth and forested surfaces are given. Each point in the colored area denotes the exposure coefficient for the chosen distance from the hill, the chosen rotor diameter and a hub height given by the point itself (z -value). As can be inferred from Fig. 6, forested surfaces enlarge in vertical and horizontal direction significantly the area of reduced wind power in the lee

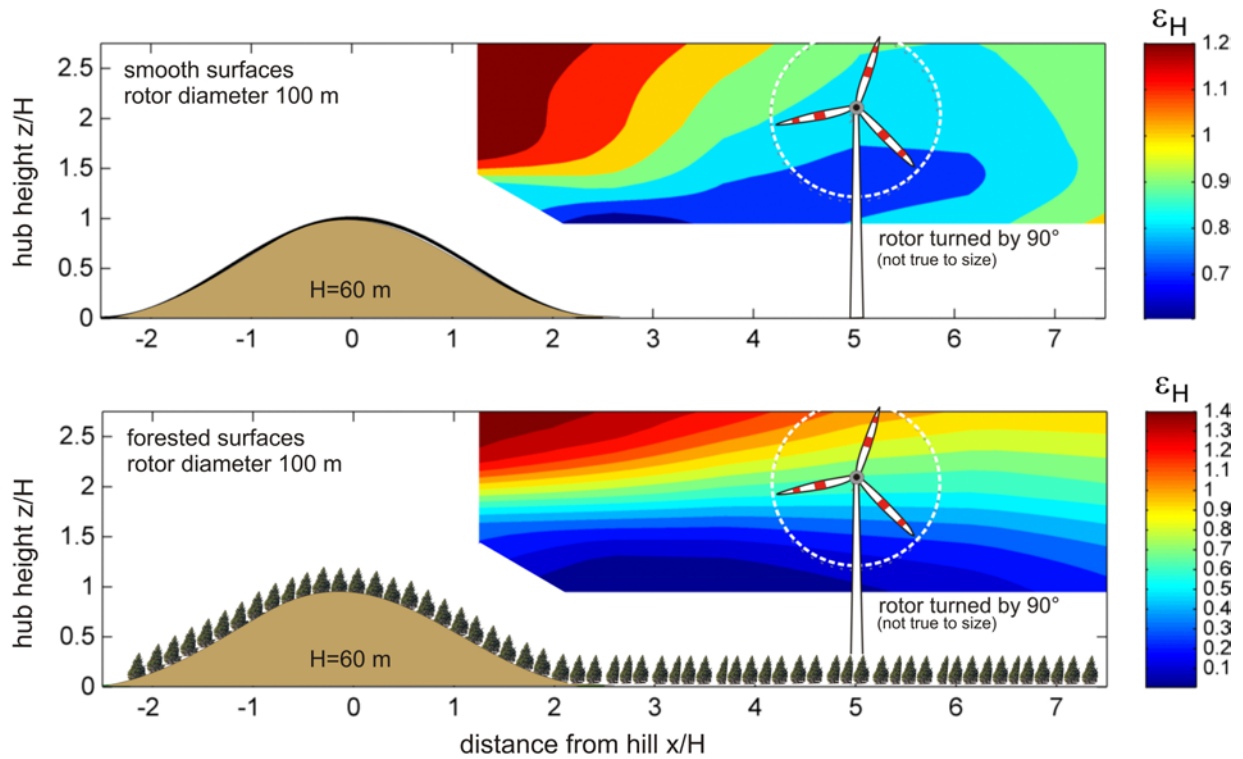


Fig. 6: Isoplots of exposure coefficients ϵ_H measured at different distances from the disturbing upstream hill (height 60 m) for varying hub heights and a fixed rotor diameter of 100 m; top: smooth surfaces; bottom: forested surfaces with tree density of 60 tree/ha, tree height 16.5 m; permeability of crown material 0.7 m^{-1}

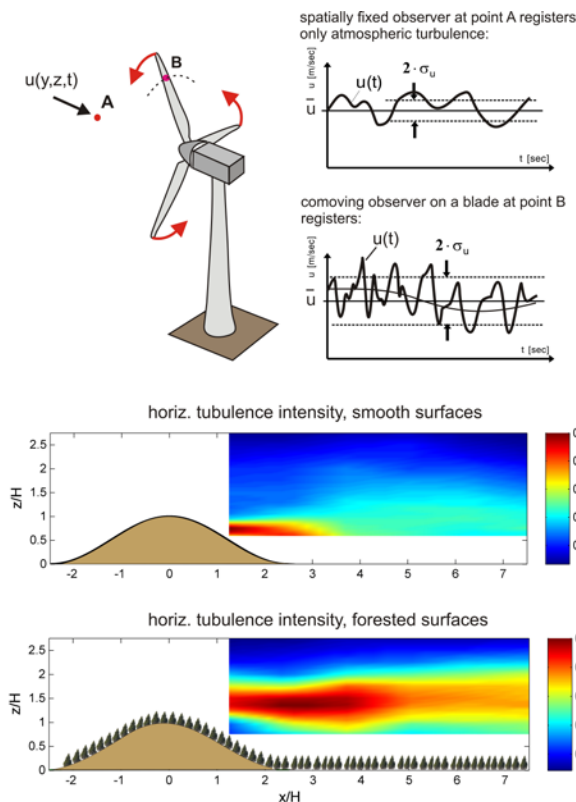


Fig. 7: Enhanced turbulent intensity due to forest canopy; hill height 60 m; top: smooth surfaces; bottom: forested surfaces; tree density 60 tree/ha, tree height 16.5 m; permeability of crown material 0.7 m^{-1}

of the hill. Whereas the boundary layer seems to recover behind the smooth hill after $x/H \approx 7-8$, the zone of reduced wind power extends far above this value for the forested case. One can also see that the wake zone thickens in vertical direction for forested surfaces, leading to a much higher hub height, when the same wind power shall be reached.

Wind turbines are subject to wind variations of different time scales, see e.g. [31]. A most important factor of influence for material fatigue is the turbulence level in which the rotor performs. The rotor blades experience an effective gustiness which is much higher than the normal atmospheric gustiness. This is due to the fact that a blade may travel through various gust during one rotation, whereas an observer fixed in space may be exposed in the same time only to one single gust. This problem is enhanced by a forested upstream hill as can be seen in Fig. 7.

As can be inferred from Fig. 7, the horizontal turbulence intensity increases strongly due to the presence of the forest canopy. Apparently, the vertical momentum exchange is intensified due to the rough and permeable structure of the canopy. The increased momentum exchange thickens the free shear layer and leads to a long-lasting increase of turbulence intensity downstream of the hill. Thus, the area of higher turbulence intensity behind the hill is enlarged in vertical and horizontal direction. For a wind turbine positioned in the lee of a forested hill, this means in terms of material fatigue for a blade that the number of crossings over a certain deflection is increasing reducing its lifetime.

V. RESULTS CONFIGURATION B

Configuration B refers to the case, where the wind turbine is positioned not in plane terrain but also on a two dimensional hill of the same size as the disturbing upstream hill, see Fig. 1 bottom. Being the most probable case in mountainous regions, we restrict the following only to forested landscape. In Figures 8 and 9, the exposure coefficients for wind turbines with rotor diameter of 80 m, 100 m and 120 m and variable hub heights are shown. Each curve refers to a specific position (dimensionless distances x/H between wind turbine hill and disturbing hill). Please note that for configuration B the dimensionless distance x/H is measured from right to left and in order to cover a longer distance range, the scale was chosen to 1:400 with hill heights of 40 m. The wind approaches from left as before.

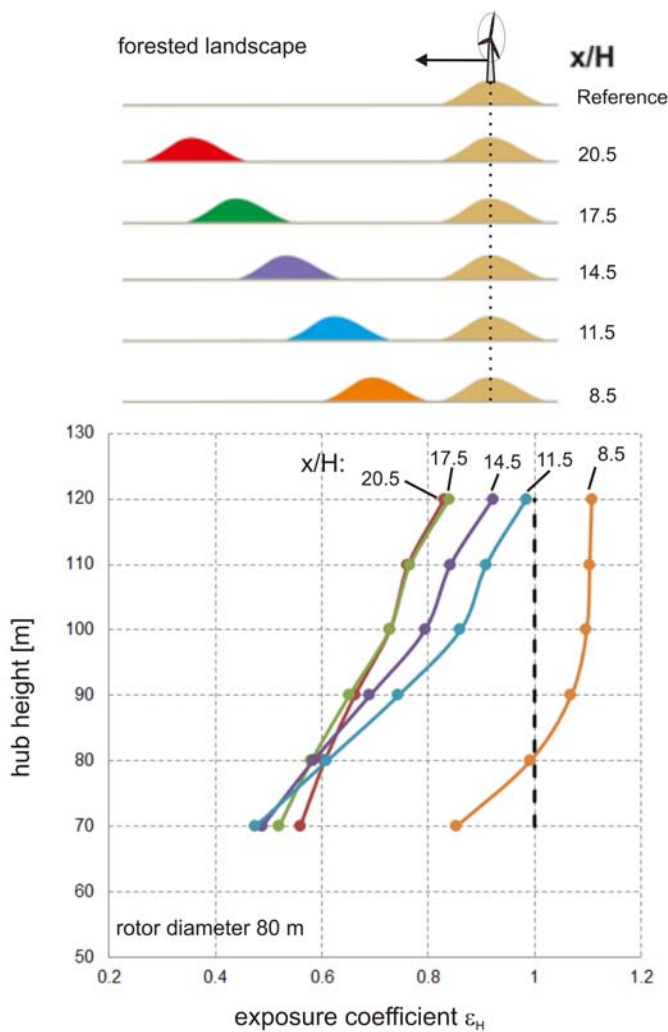


Fig. 8: Exposure coefficients ϵ_H measured at different distances of the disturbing upstream hill (height 40 m) from the wind turbine hill (height 40 m) for varying hub heights and fixed rotor diameter of 80 m; all surfaces forested with tree density of 60 tree/ha, tree height 16.5 m; permeability of crown material 0.7 m^{-1}

The interpretation of the curves in Figure 8 and 9 is similar to figure 4 and 5. Going upwards along a curve means that at

the same distance from the hill the hub height is pushed upwards, which in most cases increases the exposure coefficient. The curves stem all from velocity field measurements over the fixed wind turbine hill and only the distance of the disturbing upstream hill was varied.

First of all, one can infer from Fig. 8 and 9 that the existence of a hill in the fetch in a distance of above $x/H \approx 10$ increases the available wind power for hill-mounted wind turbines. As can be seen also for distances below $x/H \approx 10$, the exposure values can exceed 1.0, which means that the wind power is increased when compared to the reference case.

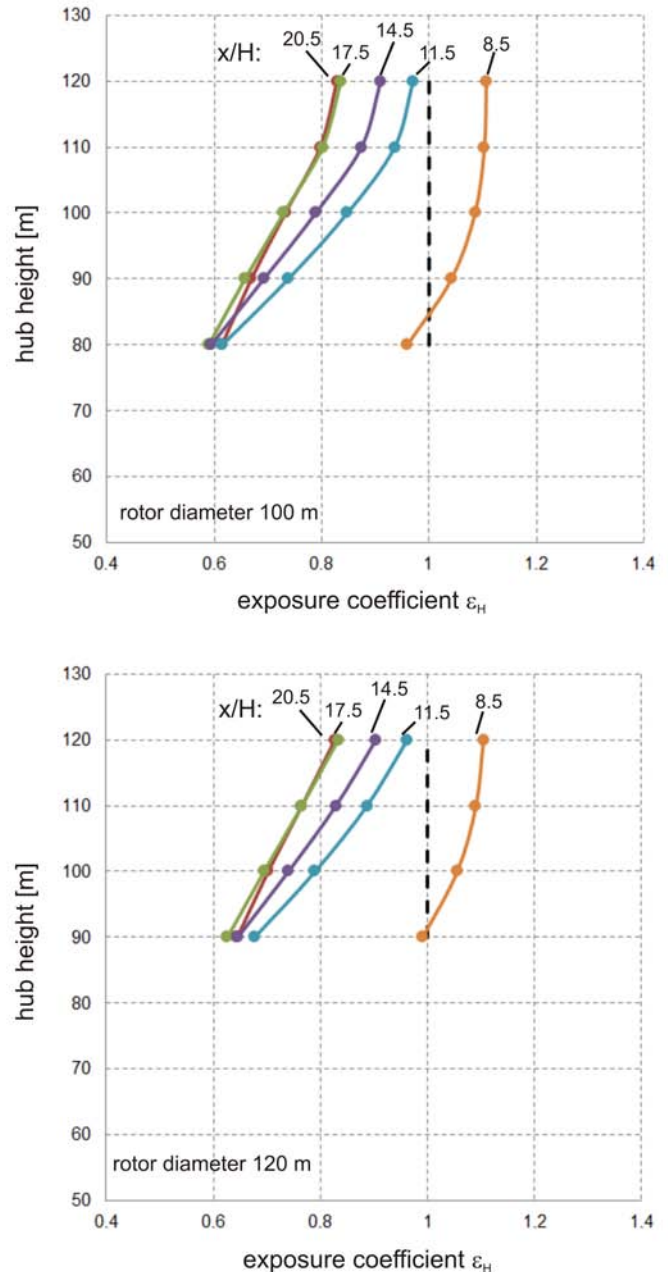


Fig. 9: Exposure coefficients ϵ_H measured at different distances of the disturbing upstream hill (height 40 m) from the wind turbine hill (height 40 m) for varying hub heights and fixed rotor diameter of 100 m (top) and 120 m (bottom); all surfaces forested with tree density of 60 tree/ha, tree height 16.5 m; permeability of crown material 0.7 m^{-1}

Looking at the tendency of wind power loss reveals that for hub heights above 80 m and distances $8.5 \leq x/H \leq 20.5$, the exposure coefficients decrease with increasing distance of the disturbing hill (or increase with decreasing distance). This means that the closer the disturbing hill the smaller is the power loss. Apparently, a very close disturbing hill ($x/H=8.5$) acts as a baffle deflecting the approaching wind upwards and increasing the wind power available for the hill-mounted wind turbine when compared to the reference case. On the other hand, the almost identical curves for $x/H=17.5$ and $x/H=20.5$ show that the loss-creating influence of the disturbing hill reaches its maximum within this distance range and it is most probable that the induced losses will decrease for longer distances, i.e. the exposure coefficients will increase for longer distances and come close to the reference value of 1.0 (distance of disturbing hill goes to infinity).

Comparing the exposure coefficients for a hub height of e.g. 100 m in the plots of Fig. 8 and 9 reveals (again) that their values do not fluctuate much and that the rotor diameter is not a factor of major influence.

For a fixed wind turbine on a hill, the rotor diameter, the hub height and the distance of a disturbing upstream hill control the wind energy efficiency in the present case. Each point of a curve in the plots of Fig. 8 and 9 represent for a chosen rotor diameter the exposure coefficients at a specific hill-to-hill distance and hub height. Instead of displaying the values of the exposure coefficients on the abscissa, one can code them in color. On the basis of the measured flow field, one can compute the exposure coefficients for all possible positions in the whole hill-to-hill distance range of $8.5 \leq x/H \leq 20.5$ and display the values in an isopleth, see Fig. 10.

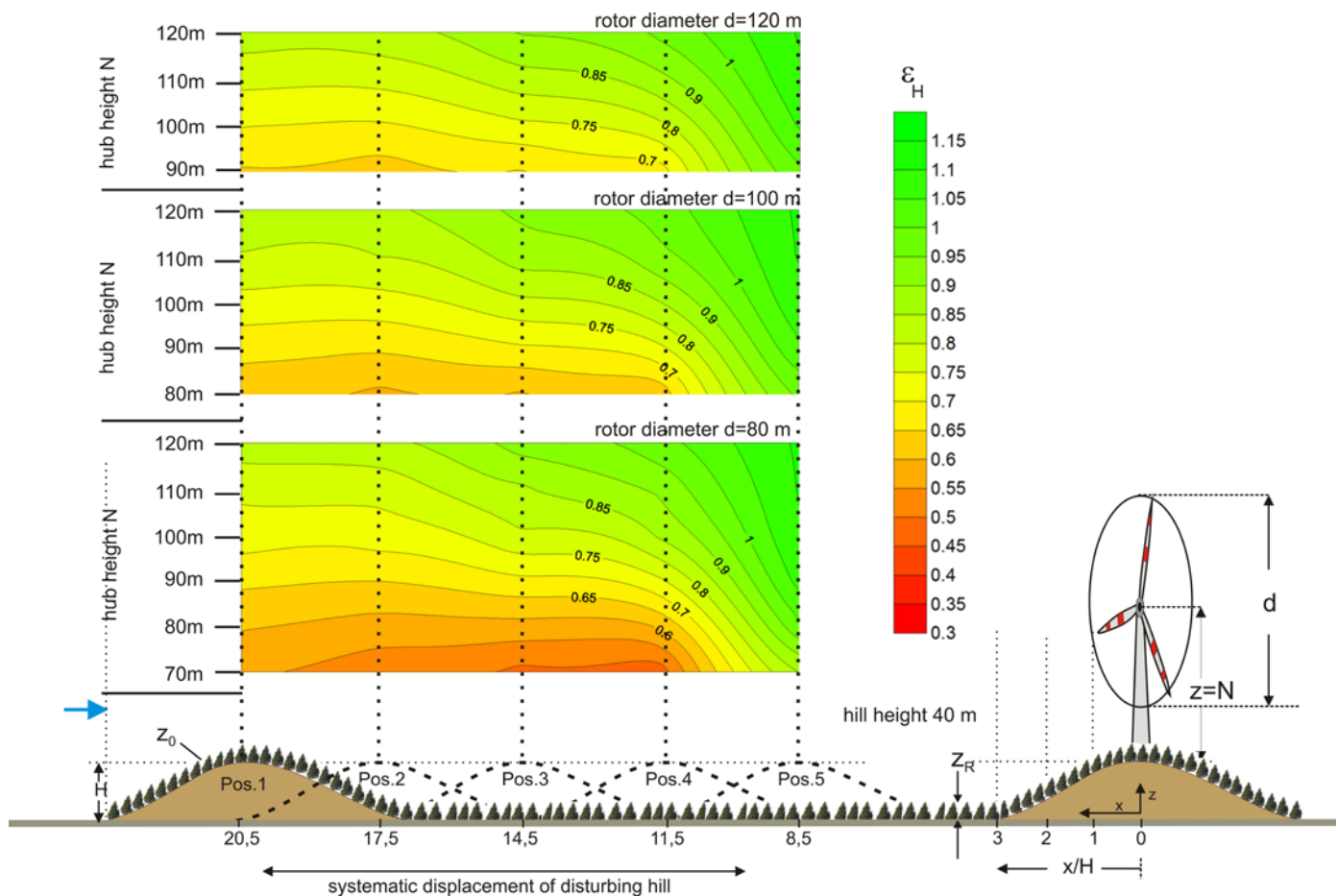


Fig. 9: Exposure coefficients ϵ_H measured at different distances of the disturbing upstream hill (height 40 m) from the wind turbine hill (height 40 m) for varying hub heights and fixed rotor diameter of 80m, 100 m and 120 m, all surfaces forested with tree density of 60 tree/ha, tree height 16.5 m; permeability of crown material 0.7 m⁻¹

VI. CONCLUSION

Experimental investigations have been carried out in an atmospheric boundary layer wind tunnel in order to clarify the interaction of wind turbines and upstream hills. The properties of an atmospheric boundary layer flow as well as realistic sur-

face roughness have been simulated. Two configurations were tested, one (A) concerning a wind turbine erected in plane countryside and the other (B) concerning of a wind turbine erected on a hill. In both configurations a disturbing hill (height: 60m and 40 m respectively) was positioned upstream and the influence was measured, which the disturbing hill exerts on the wind power available for the wind turbine. The re-

sults show that in most cases an upstream hill reduces the wind power significantly and that only in few cases, where the disturbing hill is close to the turbine and acts as a baffle, an increase in wind power can be registered. The ratio of hub height to hill height is crucial and determines whether the rotor performs at least partially in the wake of the hill or outside of the free shear layer induced by the hill. The influence of forested surfaces is very strong. When compared to smooth surfaces, roughness and permeability of the forest canopy triggers flow separation and increases the vertical momentum exchange of the surface boundary layer leading to a thickening of the free shear layer and a stronger vertical displacement of the flow. As a consequence of these processes, the available wind power is reduced drastically when compared to smooth surfaces. For configuration A, forested surfaces reduce the available wind power of 25-50 % depending on the hub height of the turbine (120 m and 90 m). The enhanced turbulent level of the wind flow induced by forested surfaces can be assessed e.g. by measuring the turbulence intensity or spectrum and is an important factor in material fatigue assessments.

When the wind turbine is erected on a hill (configuration B), the maximum loss of wind power for turbine hub heights of z/H greater than about 2 was measured at a disturbing hill distance of $17.5 \leq x/H \leq 20.5$. This implies that, obviously, a specific distance of the disturbing hill exists, which induces maximum wind power loss for the turbine.

Finally, it should be stated that the results presented here are deduced from experiments with hills of 60m and 40 m height, hub heights of 80-120 m and rotor diameters of 70-120 m. For assessment purposes of other configurations, the ratios of these quantities should be considered.

References:

- [1] Mortensen, N.G., Landberg, L., Troen, I., Petersen, E.L., Wind Atlas Analysis and Application Program (WAsP). Vol. 2: User's Guide, Risø-I-666(v.2) (EN), Risø National Laboratory, Roskilde, Denmark, 1993.
- [2] Troen, I., Petersen, E.L., European Wind Atlas, Published for the Commission of the European Communities, Brussels, Belgium, by Risø National Laboratory, Roskilde, Denmark, ISBN 87-550-1482-8, 1989.
- [3] Jackson, P.S., Hunt, J.C.R., "Turbulent wind flow over a low hill", Q. J. R. Meteorol. Soc., 101, 1975, pp. 929–955.
- [4] Anthony J. Bowen, A.J., Mortensen, N.G., "WAsP prediction errors due to site orography", Report Risø-R-995(EN), Risø National Laboratory Roskilde Denmark, 2004, ISSN 0106-2840, ISBN 87-550-2320-7
- [5] Botta, G., Castagna, R., Borghetti, M., Mantegna, D., "Wind analysis on complex terrain – The case of Acqua Spruzza", Jour. Wind Eng. Ind. Aerodyn. 39, 1992, pp. 357- 66.
- [6] Ayotte, K.W., "Computational Modelling for Wind Energy Assessment", J. Wind Eng. Ind. Aerod., 96, 2008, pp. 1571–1590.
- [7] Gravdahl AR, Harstveit K., "WindSim – Flow simulations in complex terrain, Assessment of wind resources along the Norwegian coast", Deutsche Windenergie Konferenz DEWEK, 2000.
- [8] Schmidt, T., Mockett, C., Thiele, F., "Minimization and Quantification of Errors and Uncertainties in RANS Modeling", Management and Minimisation of Uncertainties and Errors in Numerical Aerodynamics, Notes on Numerical Fluid Mechanics and Multidisciplinary Design, Volume 122, 2013, pp. 77-100
- [9] Sumner, J., Watters, C.S., Masson, C., "CFD in Wind Energy: The Virtual, Multiscale Wind Tunnel", Energies, 3, 2010, pp. 989-1013
- [10] Walmsley, J.L., Troen, I., Lalas, D.P., Mason, P.J., "Surface-layer flow in complex terrain: Comparison of models and full-scale observations", Boundary-Layer Meteorology 52, 1990, pp. 259-81.
- [11] Frenkiel, J., "Wind Profiles over Hills", Quart. J. Roy. Meteorol. Soc., 88, 1962, 156–169
- [12] Taylor, P. A., "Some Numerical Studies of Surface Boundary-Layer Flow above Gentle Topography", Boundary-Layer Meteorol. 11, 1977, 439–465.
- [13] Sykes, R. I., "An Asymptotic Theory of Incompressible Turbulent Boundary-Layer Flow over a Small Hump", J. Fluid Mech. 101, 1980, 647–670.
- [14] Mason, P. J., King, J. C., "Atmospheric Flow over a Succession of Nearly Two-Dimensional Ridges and Valleys", Quart. J. Roy. Meteorol. Soc. 110, 1984, pp. 821–845.
- [15] Taylor, P. A., Teunissen, H. W., "The Askervein Hill Project: Overview and Background Data", Boundary-Layer Meteorol. 39, 1987, 15–39
- [16] Bradley, E.F., "An experimental study of the profiles of wind speed, shearing stress and turbulence at the crest of a large hill", Quarterly Journal of the Royal Meteorological Society. 106 (447), 1980, pp. 101–123
- [17] Britter, R. E., Hunt, J. C. R., Richards, K. J., "Air Flow over a Two-Dimensional Hill: Studies of Velocity Speed-Up, Roughness Effects and Turbulence", Quart. J. Roy. Meteorol. Soc. 107, 1981, 91–110.
- [18] Finnigan, J. J., Raupach, M. R., Bradley, E. F., Aldiss, G. K., "A Wind Tunnel Study of Turbulent Flow over a Two-Dimensional Ridge", Boundary-Layer Meteorol. 50, 1990, 277–317
- [19] Pearse, J.R., "Wind flow over conical hills in a simulated atmospheric boundary layer", Journal of Wind Engineering and Industrial Aerodynamics. 10 (3), 1982, pp. 303–313
- [20] Teunissen, H.W., "Wind-tunnel and full-scale comparisons of mean wind flow over an isolated low hill", Journal of Wind Engineering and Industrial Aerodynamics. 15 (1-3), 1983, pp. 271–286
- [21] Ruck, B.; Adams, E., "Fluid mechanical aspects of the pollutant transport to coniferous trees", Boundary-Layer Meteorology. 56 (1), 1991, pp. 163–195
- [22] Neff, D. E., Meroney, R. N., "Wind-tunnel modeling of hill and vegetation influence on wind power availability", Journal of Wind Engineering and Industrial Aerodynamics. 74-76 (0), 1998, pp. 335–343

- [23] Houra, T.; Nagano, Y., "Turbulent heat and fluid flow over a two-dimensional hill", *Flow, Turbulence and Combustion*. 83 (3), 2009, pp. 389–406
- [24] Focken U, Heinemann D, "Influence of thermal stratification on wind profiles for heights up to 140 m", *Proceedings of the European Wind Energy Conference*, Madrid, 2003.
- [25] Poullikkas, A., Kourtis, G., Hadjipaschalis, I., "An overview of the EU Member States support schemes for the promotion of renewable energy sources", *Int. Journal of Energy and Environment*, Volume 3, Issue 4, 2012, pp. 553-566
- [26] Meroney, R. N., "Characteristics of Wind and Turbulence in and above Model Forests", *J. Appl. Meteorol.*, 7, 1968, pp. 780-788
- [27] Counihan, J., "Wind tunnel determination of the roughness length as a function of the fetch and the roughness density of three-dimensional roughness elements", *Atmospheric Environment*, 5 (8), 1971, pp. 637– 642.
- [28] Plate, E.J., "Wind tunnel modelling of wind effects in engineering", *Engineering Meteorology*, (edited by Plate E.J.), Elsevier, 1982, pp. 573–640.
- [29] Gromke, C., Ruck, B., "Aerodynamic modeling of trees for small scale wind tunnel studies", *Forestry*, 2008, Volume 81, Issue 3, pp. 243-258
- [30] Ruck, B., Frank, C., Tischmacher, M., "On the influence of windward edge structure and stand density on the flow characteristics at forest edges", *European Journal of Forest Research*, 131, 2012, pp. 177–189.
- [31] Tarquis, A.M., Morató, M.C., Castellanos, M.T., De Miguel, J.L., "Wind Velocity Fluctuations Time Series Analysis", *Proc. of the 5th WSEAS Int. Conf. on Signal Processing, Robotics and Automation*, Madrid, Spain, 2006, pp. 268-272